Inconsistencies between satellite estimates of longwave cloud forcing and dynamical fields from reanalyses

Richard P. Allan[1] and Mark A. Ringer
Hadley Centre, Met Office, Bracknell, Berkshire, UK

Received 30 January 2003; revised 15 April 2003; accepted 17 April 2003; published 15 May 2003.

[1] The greenhouse effect of cloud may be quantified as the difference between outgoing longwave radiation (OLR) and its clear-sky component (OLRc). Clear-sky measurements from satellite preferentially sample drier, more stable conditions relative to the monthly-mean state. The resulting observational bias is evident when OLRc is stratified by vertical motion; differences to climate model OLRc of 15 Wm^{-2} occur over warm regions of strong ascent. Using data from the ECMWF 40-year reanalysis, an estimate of cloud longwave radiative effect is made which is directly comparable with standard climate model diagnostics. The impact of this methodology on the cancellation of cloud longwave and shortwave radiative forcing in the tropics is estimated. *INDEX TERMS:* 1620 Global Change: Climate dynamics (3309); 1640 Global Change: Remote sensing; 1694 Global Change: Instruments and techniques; 3359 Meteorology and Atmospheric Dynamics: Radiative processes; 3360 Meteorology and Atmospheric Dynamics: Remote sensing. **Citation:** Allan, R. P., and M. A. Ringer, Inconsistencies between satellite estimates of longwave cloud forcing and dynamical fields from reanalyses, *Geophys. Res. Lett.*, *30*(9), 1491, doi:10.1029/2003GL017019, 2003.

1. Introduction

[2] Accurate prediction of future climate demands an adequate representation of mechanisms responsible for the present day distribution and variability of clouds and water vapor and their resulting radiative impacts [*Intergovernmental Panel on Climate Change*, 2001]. Satellite measurements of the Earth's radiative energy balance present one method of evaluating the physical processes currently depicted in climate models [e.g., *Cess et al.*, 1997; *Allan and Slingo*, 2002] and also provide insight into the subtle relationships between the hydrological cycle, the radiation budget and the dynamics of the atmosphere [*Kiehl*, 1994; *Hartmann et al.*, 2001].

[3] An important advance in quantifying the observed cloud radiative effect was made possible by the sub-sampling of clear-sky fluxes from the Earth Radiation Budget Experiment (ERBE [*Barkstrom et al.*, 1989]) and the calculation of cloud radiative forcing as the difference between the clear-sky and all-sky fluxes [e.g., *Ramanathan et al.*, 1989]. More recently, the value of analysing the radiation budget in terms of dynamical parameters, such as mean vertical motion, has further improved our understanding of the climate system [e.g., *Bony et al.*, 1997; *Allan et al.*, 2002b]. However, it has long been recognised that the cloud radiative forcing measured by satellites is inconsistent with that generally produced as standard output from climate models [*Cess and Potter*, 1987]. In climate models, clear-sky fluxes are usually calculated diagnostically at every time-step by setting cloud amount to zero in the radiation scheme. Clear-sky measurements from satellite are made only for pixels that are deemed to be free of cloud cover. We argue that monthly mean clear-sky outgoing longwave radiation (OLRc) measurements are inconsistent with the mean vertical motion fields. Therefore, evaluation of climate models and quantification of cloud radiative effect in terms of the monthly mean vertical motion may provide misleading results. We combine reanalysed OLRc from the European Centre for Medium Range Weather Forecasts (ECMWF) with observed all-sky outgoing longwave radiation (OLR) to overcome the sampling problems in the calculation of cloud longwave radiative effect.

2. Longwave Cloud Radiative Forcing

[4] Longwave cloud radiative forcing (LWCF) is computed:

$$LWCF = OLRc - OLR. \quad (1)$$

Differences in cloudiness between climate models and satellite data will cause associated differences in OLR and hence LWCF. However, if OLRc is significantly different between models and data, the model-observation difference in LWCF will not directly relate to the contrasting radiative effects of cloud. Satellite instruments cannot measure OLRc over cloudy, moist regions. Because these regions tend to produce the lowest OLRc in the model calculations, there exists an observed minus model positive OLRc bias in monthly-mean products relating to the disparate sampling of clear-sky fluxes [*Cess and Potter*, 1987].

[5] Figure 1 shows the LWCF and OLRc differences for the Hadley Centre atmosphere-only climate model (HadAM3 [*Pope et al.*, 2000]) minus observations from the Earth Radiation Budget Satellite, ERBS (primary ERBE satellite). The HadAM3 simulations, which were forced by the observed sea surface temperature (SST) and sea-ice distributions over the period 1978–99, are described in *Allan et al.* [2003]. HadAM3 underestimates LWCF over tropical convective regions compared to ERBS, in part due to an underestimation of cloud greenhouse effect [*Allan et al.*, 2002b]. However, Figure 1b shows differences in model minus observed OLRc greater in magnitude than 10 Wm^{-2}. In particular, OLRc differences over the South Pacific are larger than the LWCF differences. *Allan et al.* [2003] showed reduced OLRc differences when the model sampled clear-

[1]Now at Environmental Systems Science Centre, University of Reading, Reading, Berkshire, UK.

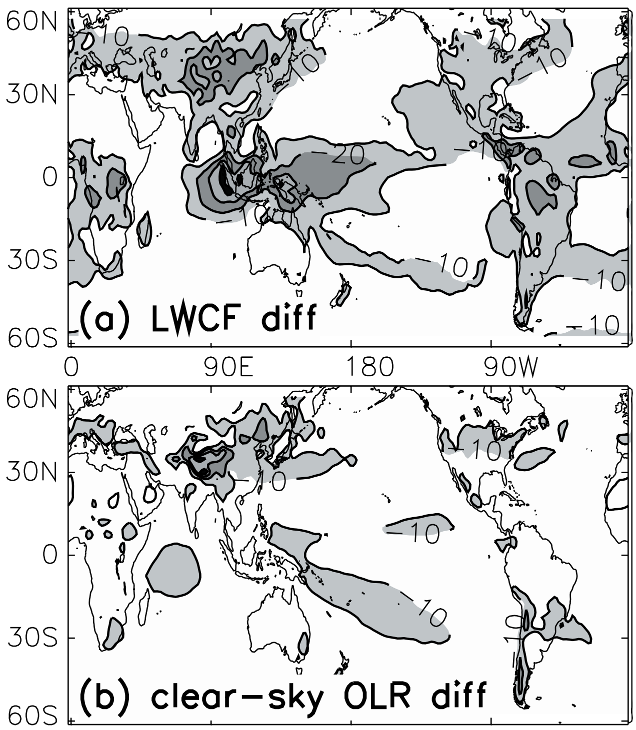

Figure 1. HadAM3 minus ERBS (a) longwave cloud radiative forcing and (b) clear-sky OLR for 1985–89. Values less than −10 Wm^{-2} are shaded (contour interval: 10 Wm^{-2}).

sky fluxes in a manner more consistent with the satellite data (Type-I) compared to the standard model diagnostic (Type-II). Regardless of the source of OLRc disparity between models and satellite data, it is clear that differences in LWCF cannot be related to differences in cloud properties alone.

3. Clear-Sky OLR Stratified by Vertical Motion and Sea Surface Temperature

[6] Many of the differences in Figure 1 are related to the inconsistent locations of the dry or the moist regions between the model and observations. While it is important to reproduce the observed climatological distribution of clouds and water vapor, it is equally important to simulate the correct radiative effect of a given dynamical regime. Further, differences in spatial location of convection or subsidence can confuse the interpretation of the differences due to model errors in cloud or atmospheric properties. Previous studies have shown the value of using vertical motion fields from reanalyses to aid the interpretation of cloud radiative forcing comparisons between models and observations [e.g., *Bony et al.*, 1997]. Here we use the method described by *Williams et al.* [2003], in which we calculate the mean OLRc in bins of 500 hPa vertical motion (ω) and SST.

[7] Figure 2 shows OLRc in ω-SST bins for ERBS and HadAM3 over the oceans. We use ω and SST from the ECMWF 15-year reanalysis (ERA-15 [*Gibson et al.*, 1997]) to sub-sample ERBS. The population of each bin (contour lines) peaks at ω ~ 0, particularly at SST = 300 *K*. The lowest OLRc values occur at the coldest SSTs and the highest OLRc occurs over warm SSTs for positive ω (descent). Over warm regions of strong ascent (ω < 0; SST > 295 *K*), the OLRc simulated by HadAM3 is in the range 260–280 Wm^{-2} while the corresponding observed values are generally greater than 280 Wm^{-2}. The HadAM3 minus ERBS difference is displayed in Figure 2c. Large negative differences of −15 Wm^{-2} occur over warm, ascending regions, although differences of −5 to −10 Wm^{-2} also predominate over cooler SSTs. Over warm, descending regions, where cloud cover and hence clear-sky sampling differences between model and satellite data are small, OLRc differences are also small. Differences in population across the bins (contour lines) show the model to have more strong ascent and strong descent than the reanalysis over warm oceans. This is symptomatic of an over-active large-scale circulation in HadAM3, consistent with previous findings [*Pope et al.*, 2000].

[8] The OLRc difference pattern can be explained by the clear-sky sampling. Clear-sky satellite measurements are possible only for effectively cloud-free pixels; where no clear-sky pixels are available, a value is prescribed where possible using interpolation. Cloud-free times generally

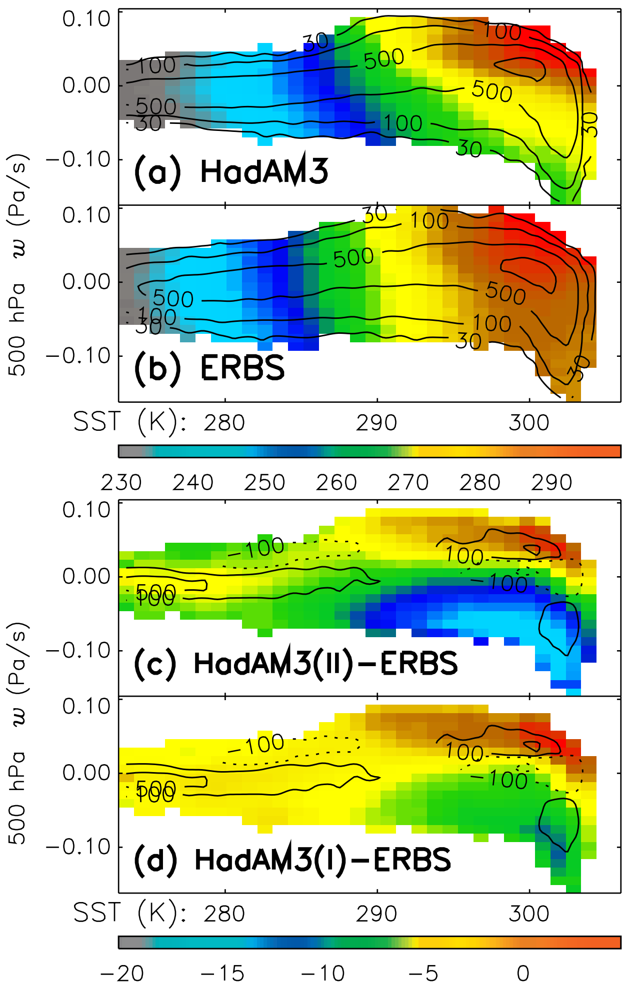

Figure 2. OLRc (Wm^{-2}; color bar) with 500 hPa ω (10 hPa/day bins) and SST (1 *K* bins) for 1985–89, 60°N–60°S: (a) HadAM3 (Type II), (b) ERBS, and HadAM3 minus ERBS OLRc difference (Wm^{-2}; color bar) for (c) Type-II and (d) Type-I model fluxes. Contour lines denote the number of grid points in each bin or their difference.

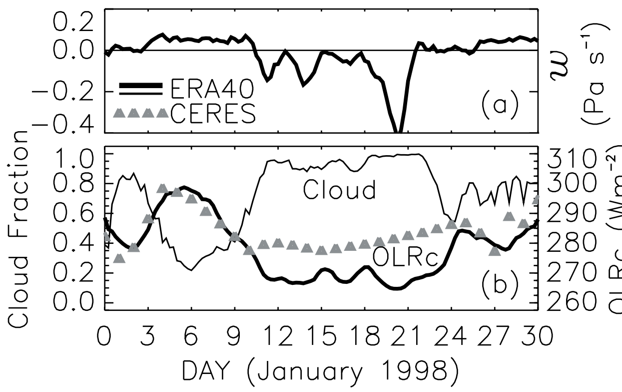

Figure 3. Daily 500 hPa ω, cloud fraction and OLRc from ERA-40 and CERES OLRc for 230°E, 15°S, January 1998.

correspond with weaker ascent relative to monthly-mean ω. This is illustrated using daily data from a new 40-year ECMWF reanalysis (ERA-40 [*Chevallier et al.*, 2001]) over the south Pacific (Figure 3); similar results apply at other locations. The most cloudy period (days 10–20) corresponds with the lowest OLRc and anomalously negative ω. Also plotted is colocated daily OLRc data from the Clouds and the Earth's Radiant Energy System (CERES [*Wielicki et al.*, 1996]) satellite instrument. There is excellent agreement between ERA-40 and CERES data for $\omega \geq 0$. However, during the overcast period ($\omega < 0$) CERES OLRc appears higher than ERA-40 due to interpolation of the satellite data between clear points. Thus, the monthly OLRc observations represent more positive vertical motion than the monthly-mean ω. This may explain the lack of OLRc variation with ω for ERBS (Figure 2b) compared with HadAM3 (Figure 2a). Sampling HadAM3 OLRc in a manner more consistent with the satellite data (Type-I), the OLRc differences to ERBS (Figure 2d) are much reduced compared to Figure 2c. We approximated the satellite subsampling by weighting OLRc with clear-sky fraction [see *Allan et al.*, 2003] thereby effectively biasing the data towards clear-sky times at each grid point. Because the satellite pixels are much smaller than model grid-boxes, it is difficult to completely remove the sampling disparity. Differences in pixel sizes between satellite instruments may also cause a sampling bias.

4. Using ERA-40 OLRc to Calculate LWCF

[9] Avoiding satellite clear-sky sampling errors is possible by comparing all-sky fluxes [e.g., *Allan and Slingo*, 2002] although cloud radiative effect may only be inferred. Using satellite-like sampling of OLRc (Type-I) also provides a more consistent comparison between models and observations but does not circumvent the inconsistency between LWCF and monthly mean ω. Another possibility is to combine OLRc from reanalyses with satellite OLR to calculate LWCF. Reanalysis data has the following advantages: (i) clear-sky sampling is consistent with climate models, (ii) the realistic large-scale circulation is spatially consistent with observed radiation budget data, (iii) the reanalysis contains observationally-based information on the atmospheric state. *Slingo et al.* [1998] used ERA-15 data to produce simulations of the clear-sky radiation budget, including OLRc, for 1979–93. While erroneous humidity variations reduced the value of ERA-15, moisture fluctuations are improved in ERA-40 [*Allan et al.*, 2002a]. Further comparisons with other reanalyses and observations (e.g., Figure 3) are required to demonstrate the quality of ERA-40 OLRc.

[10] Figure 4 shows the 40°S–40°N OLRc for 1998 with mean ω and SST for HadAM3, ERA-40 and CERES satellite data. As in Figure 2, the HadAM3 and satellite data show large differences, particularly over warm, ascending regions. The ERA-40 OLRc (Figure 4c) shows small differences to the satellite data away from strong ascent (Figure 4d). However, ERA-40 produces OLRc below 280 Wm^{-2} over the warm, convecting regions which is consistent with the model data and about 8 Wm^{-2} lower than CERES.

[11] Finally, we use ERA-40 OLRc to assess the near-cancellation of shortwave and longwave radiative effects of cloud over the deep tropics [e.g., *Kiehl*, 1994]. Considering data for April 1998 over the equatorial Pacific (10°S to 10°N) we plot the difference in LWCF due to the model minus satellite sampling discrepancy against the shortwave cloud radiative forcing (SWCF: clear-sky minus all-sky reflected shortwave radiation at the top of the atmosphere). In Figure 5a, the difference is calculated as CERES/ERA40 LWCF minus CERES LWCF. In Figure 5b the difference is

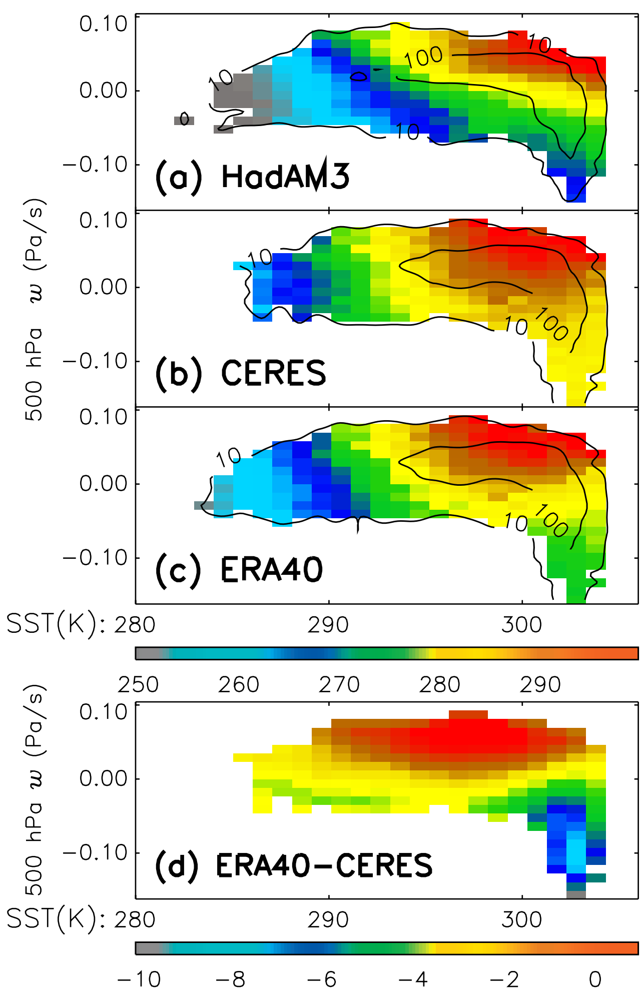

Figure 4. Clear-sky OLR plotted with bins of 500 hPa ω and SST for 40°S–40°N for (a) HadAM3, (b) CERES, (c) ERA40 and (d) ERA40-CERES for January–August 1998. Contours denote the number of grid points within each bin.

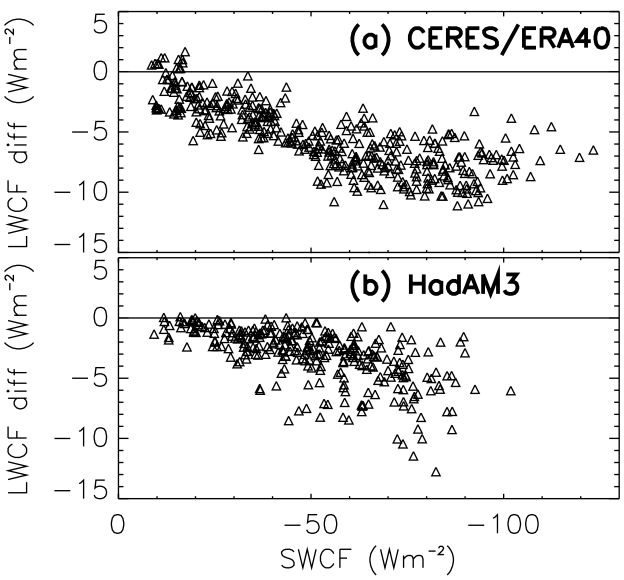

Figure 5. Difference in LWCF (Wm^{-2}) for (a) CERES/ERA40 minus CERES-only and (b) HadAM3 Type II minus HadAM3 Type I plotted with SWCF (Wm^{-2}) for April 1998 (10°S–10°N, 140–270°E).

HadAM3 Type-II LWCF minus HadAM3 Type-I (satellite-like) LWCF. In Figures 5a and 5b the magnitude of LWCF difference increases with the magnitude of SWCF. This is consistent with Figures 2 and 4 in which the largest sampling errors are associated with warm, convective regimes which also correspond with the strongest SWCF. For the CERES/ERA40 method (Figure 5a), the gradient of the regression between LWCF difference and SWCF is 0.13 with a correlation coefficient, r = 0.77. Thus, using the satellite data only will overestimate LWCF for the strongest SWCF. For the equatorial Pacific, the observed regression gradient, $\frac{d(-SWCF)}{dLWCF} = 1.20$ (r = 0.95), is increased to $\frac{d(-SWCF)}{dLWCF} = 1.33$ (r = 0.95) when using ERA-40 OLRc. Inconsistent clear-sky sampling will also cause the ratio, $-SWCF/LWCF$ [e.g., *Kiehl*, 1994], to be underestimated over convective regions by satellite data compared to models. These relationships will also be affected by the satellite sampling of SWCF which are not discussed here.

5. Summary

[12] The monthly-mean LWCF derived from satellite data is inconsistent with monthly-mean dynamical fields. Because clear pixels are biased towards descent or weak ascent, the analysis of cloud radiative effect as a function of dynamical regime may produce misleading results. Sampling errors are identified by stratifying OLRc by mean vertical motion and SST. The largest satellite-model differences of ~15 Wm^{-2} occur over warm, ascending regimes. These differences are much reduced when the climate model data is sampled in a way more consistent with satellite data. We use reanalysis OLRc from ERA-40 in conjunction with the satellite all-sky OLR as an alternative method of calculating LWCF. The reanalysis data samples OLRc in a manner consistent with monthly mean ω and climate model clear-sky diagnostics. ERA40 also provides a realistic spatial distribution of the large-scale circulation and contains observationally based information on the state of the atmosphere. Away from strong ascent ERA-40 OLRc compares favourably with satellite data. Using ERA-40 and CERES data, we suggest that satellite data may underestimate the gradient $\frac{d(-SWCF)}{dLWCF}$ over the equatorial Pacific. However, further analysis is required to establish the quality of ERA-40 OLRc.

[13] **Acknowledgments.** The ERBE and CERES data were retrieved from the NASA Langley DAAC. The work was supported by the UK Department for Environment, Food and Rural Affairs contract, PECD 7/12/37 and European Union contract EVK2-CT-1999-00027. An anonymous reviewer and J.-J. Morcrette are thanked for their contribution.

References

Allan, R. P., and A. Slingo, Can current climate model forcings explain the spatial and temporal signatures of decadal OLR variations?, *Geophys. Res. Lett.*, *29*(7), 1141, doi:10.1029/2001GL014620, 2002.

Allan, R. P., A. Slingo, and V. Ramaswamy, Analysis of moisture variability in the European Centre for Medium-Range Weather Forecasts 15-year reanalysis over the tropical oceans, *J. Geophys. Res.*, *107*(D15), 4230, doi:10.1029/2001JD001132, 2002a.

Allan, R. P., A. Slingo, and M. A. Ringer, Influence of dynamics on the changes in tropical cloud radiative forcing during the 1998 El Niño, *J. Clim.*, *15*, 1979–1986, 2002b.

Allan, R. P., M. A. Ringer, and A. Slingo, Evaluation of moisture in the Hadley Centre Climate Model using simulations of HIRS water vapour channel radiances, *Q. J. R. Meteorol. Soc.*, accepted, 2003.

Barkstrom, B., E. Harrison, G. Smith, R. Green, J. Kibler, R. Cess, and the ERBE Science Team, Earth Radiation Budget Experiment (ERBE) archival and April 1985 results, *Bull. Am. Meteorol. Soc.*, *70*, 1254–1262, 1989.

Bony, S., K.-M. Lau, and Y. C. Sud, Sea surface temperature and large-scale circulation influences on tropical greenhouse effect and cloud radiative forcing, *J. Clim.*, *10*, 2055–2077, 1997.

Cess, R. D., and G. L. Potter, Exploratory studies of cloud radiative forcing with a general circulation model, *Tellus, Ser. A*, *39*, 460–473, 1987.

Cess, R. D., et al., Comparison of the seasonal change in cloud-radiative forcing from atmospheric general circulation models and satellite observations, *J. Geophys. Res.*, *102*, 16,593–16,603, 1997.

Chevallier, F., P. Bauer, G. Kelly, C. Jakob, and T. McNally, Model clouds over oceans as seen from space: Comparison with HIRS/2 and MSU radiances, *J. Clim.*, *14*, 4216–4229, 2001.

Gibson, J. K., P. Kållberg, S. Uppala, A. Nomura, A. Hernandez, and E. Serrano, ERA description: ECMWF re-analysis project report series, *ERA Proj. Rep. 1*, 72 pp., Eur. Cent. for Medium-Range Weather Forecasts, Reading, U. K., 1997.

Hartmann, D. L., L. A. Moy, and Q. Fu, Tropical convection and the energy balance at the top of the atmosphere, *J. Clim.*, *14*, 4495–4511, 2001.

Intergovernmental Panel on Climate Change, *Climate Change 2001: The Scientific Basis*, edited by J. T. Houghton et al., 881 pp., Cambridge Univ. Press, New York, 2001.

Kiehl, J. T., On the observed near cancellation between longwave and shortwave cloud forcing in tropical regions, *J. Clim.*, *7*, 559–565, 1994.

Pope, V. D., M. L. Gallani, P. R. Rowntree, and R. A. Stratton, The impact of new physical parametrizations in the Hadley Centre Climate Model—HadAM3, *Clim. Dyn.*, *16*, 123–146, 2000.

Ramanathan, V., R. D. Cess, E. F. Harrison, P. Minnis, B. R. Barkstrom, E. Ahmad, and D. Hartmann, Cloud-radiative forcing and climate: Results from the Earth Radiation Budget Experiment, *Science*, *243*, 57–63, 1989.

Slingo, A., J. A. Pamment, and M. J. Webb, A 15-year simulation of the clear-sky greenhouse effect using the ECMWF re-analyses: Fluxes and comparisons with ERBE, *J. Clim.*, *11*, 690–708, 1998.

Wielicki, B. A., B. R. Barkstrom, E. F. Harrison, R. B. Lee, G. L. Smith, and J. E. Cooper, Clouds and the Earth's Radiant Energy System (CERES): An Earth observing system experiment, *Bull. Am. Meteorol. Soc.*, *77*, 853–868, 1996.

Williams, K. D., M. A. Ringer, and C. A. Senior, Evaluating the cloud response to climate change and current climate variability, *Clim. Dyn.*, in press, 2003.

R. P. Allan, Environmental Systems Science Centre, University of Reading, 3 Earley Gate, Reading, Berkshire RG6 6AL, UK. (rpa@mail.nerc-essc.ac.uk)

M. A. Ringer, Hadley Centre, Met Office, London Road, Bracknell, Berkshire RG12 2SY, UK.